

# Weber’s law based perception and the stability of animal groups

Andrea Perna<sup>1</sup> and Jean-Louis Deneubourg<sup>2</sup>

<sup>1</sup>Department of Life Sciences, University of Roehampton, London SW15 4JD, UK

<sup>2</sup>Université Libre de Bruxelles, Campus de la Plaine, Boulevard du Triomphe, B-1050 Bruxelles, Belgium

## Abstract

Group living animals form aggregations and flocks that remain cohesive in spite of internal movements of individuals. This is possible because individual group members adjust their position and direction of movement in response to the position and motion of other group members. Recent literature has focused on elucidating these ‘interaction rules’ that mediate group coordination for different animal species empirically from tracking data of real animal groups. Here, we adopt a complementary theoretical approach and we start by considering how the spatial organisation of a group would change in the complete absence of interactions. In this condition, the group would disperse and its collective behaviour would be described in terms of a simple diffusion process. We can hence address the inverse theoretical problem of finding the individual level interaction responses that are precisely required to counterbalance diffusion and preserve group stability. We show that an individual-level response to neighbour densities in the form of a Weber’s law (a response to gradient normalised over local density) results in an ‘anti-diffusion’ term at the group level. On short time scales, this anti-diffusion restores the initial group configuration in a way which is reminiscent of methods for image deblurring in image processing. We further show that any non-homogeneous, spatial density distribution can be preserved over time if individual movement patterns have the form of a Weber’s law response. Our study identifies a general form underlying all collective animal interaction rules and points to a link between collective interactions and the fundamental functioning of perceptual systems.

## Introduction

Gregarious and social animals are capable of forming aggregations and flocks that maintain a relatively stable global configuration in spite of individual animals joining or leaving the group and continuously changing their position relative to each other. Examples of such aggregations span the whole animal kingdom from molluscs (e.g. [1]), to insects (e.g. [2]) and crustacea (e.g. [3]) to vertebrates (reviewed in [4]). If these groups can remain cohesive and maintain a stable, coherent organisation over time, this is possible because each member of the group continuously tracks the position or density of its surrounding neighbours and implements appropriate ‘response rules’ that effectively preserve group stability.

A large number of recent empirical studies has aimed at identifying the individual-level responses that mediate group formation and stability in different animal species [5, 6, 7, 8, 9, 10]. Together, these studies have supported the idea that group formation requires at least some form of inter-individual attraction. However, different studies have pointed to different attraction rules in different species, such as for instance attraction directed to one single individual at a time or simultaneously to multiple neighbours, relevant neighbours selected based on metric or topological distance, etc.

The problem is compounded by the fact that the interaction responses of animals of different species ultimately depend on the sensory modalities mediating the interaction (vocal calls, vision, pheromones), and on the underlying neural circuits involved, which are inevitably different from one species to another. In fact, there is a large variability across the sensory systems of different animals, with only very few ‘perceptual laws’ that are

shared both across taxa and across sensory modalities. One such ‘universal’ psychophysical law is the Weber-Fechner law [11], which states that the ability of a sensory system to discriminate between two physical quantities decreases in inverse proportion to the magnitude of the quantities being compared. To make an example, we can easily tell the difference between a cluster of five objects and a cluster of eight, but we cannot as easily identify the difference between -say- a cluster of 55 and one of 58 [12]. Weber’s law has been established for humans as well as for a wide range of animals ranging from ants [13], to fish[14], to corvids [15], and to primates[16] and occurs in different sensory modalities. Because Weber’s law controls the ability of animals to ‘count’ the number of neighbours in different directions, it could likely play a role also in collective aggregation phenomena.

Here, we adopt a theoretical approach towards understanding the rules of interaction that mediate the stability of animal groups: instead of trying to observe and quantify interactions for a given animal species, we consider the theoretical problem of an animal group whose member individuals *do not* interact. In the absence of interactions, the dynamics of the group is dominated by diffusion processes which can be accurately characterised in terms of Fick’s diffusion equations [17] under simple assumptions of random motion and absence of interactions. We can hence address the inverse theoretical problem of finding which individual-level interaction rules are required to precisely counter-balance the effects of diffusion and preserve group stability.

## Evolution of densities in the absence of interactions

In the absence of interactions, the movement in a random direction of individuals results in a change of densities over time that is well described by the diffusion equation [17]. Here we recall it briefly for the one dimensional case (the problem is analogous in a higher dimensional space).

For convenience, we imagine the space to be subdivided in cells of equal width  $\Delta x$  and we indicate with  $C(x, t)$  the density of individuals (e.g. number of indi-

viduals over volume of the cell) at the position  $x$  and time  $t$  (fig. 1). We focus on density, not on the absolute number of individuals, so that our quantities do not scale with the size of the cells. Within a certain time interval  $\Delta t$  a fraction  $2D$  of the individuals present in each cell move to the adjacent cells. This determines the following equation for the evolution of  $C$ :

$$C(x, t + \Delta t) = C(x, t) + D [-2C(x, t) + C(x + \Delta x, t) + C(x - \Delta x, t)] \quad (1)$$

where the density at some position  $x$  depends on the previous density at the same position, minus the fraction of individuals that moved to the neighbour cells, plus the individuals that moved into the cell from the neighbouring ones. In the limit for  $\Delta t$  and  $\Delta x$  small, equation 1 becomes

$$\frac{\partial C}{\partial t} = D' \frac{\partial^2 C}{\partial x^2} \quad (2)$$

where  $D' = D \frac{(\Delta x)^2}{\Delta t}$  (see section 0.3 for a derivation).

The solution of the diffusion equation is

$$C(x, t) = C(x, 0) * G(0, \sqrt{t}) \quad (3)$$

whereby the initial distribution  $C(x, 0)$  is convolved with a Gaussian  $G(0, \sqrt{t})$  that becomes larger and larger in time. In practice, it is as if the initial distribution was replaced by an increasingly ‘blurred’ version of itself.

## Individual-level responses based on Weber’s law produce collective-level anti-diffusion

Weber’s law states that the perceptual ability of an animal to discriminate between sensory stimuli of different intensity is directly proportional to the difference of intensity and inversely proportional to the local value of intensity. If the ability of an individual animal to discriminate densities of neighbours in different directions follows Weber’s law, we can investigate how this type of response would affect local concentrations in the same one-dimensional discretised example of figure 1

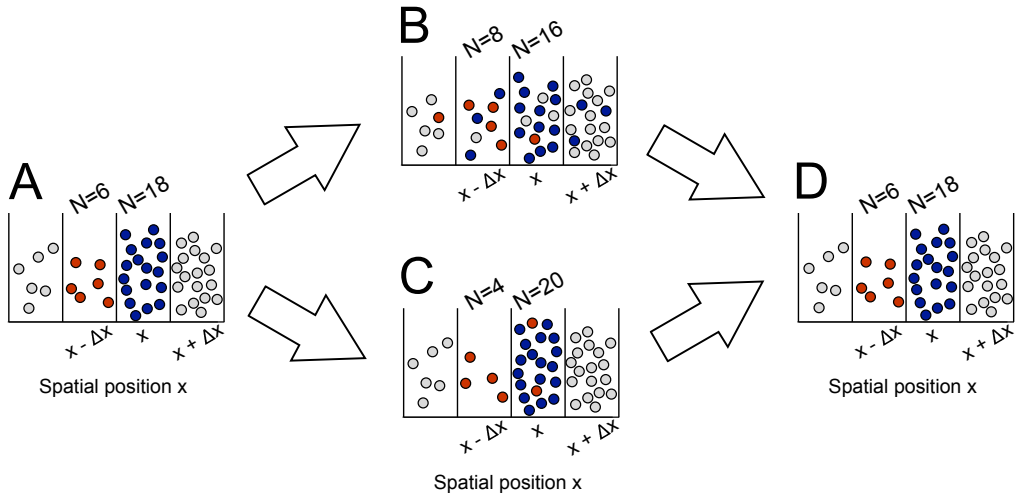


**Figure 1: Diffusion and anti-diffusion in a discrete space.** (A and B) Diffusion: each particle taking part to the initial distribution in A has a constant probability  $D$  of moving to the adjacent cell on the left, and an equal probability of moving to the cell on the right. If -as it is the case in this example- the probability is set to  $D = 1/6$ , three particles will move on average from cell  $x$  to cell  $x - \Delta x$  and on average one particle will move in the opposite direction from  $x - \Delta x$  to  $x$ . While individual particles do not show any directional preference, and they do not interact in any way, the overall process produces in this example a net flow of two particles from the region of higher concentration  $x$  to the region of lower concentration  $x - \Delta x$ . (A and C) Anti-diffusion based on Weber's Law: here each particle has a probability of moving against the concentration gradient that is proportional to Weber's contrast. If the proportionality constant is set to  $\gamma = 1/6$ , two particles on average will move from  $x - \Delta x$  to  $x$ . (D) If both diffusion and anti-diffusion take place simultaneously the net effect is that of stabilising group configuration.

(see also section 0.3 for another intuitive justification for the choice of focusing on Weber's law). In order to contrast diffusion, each individual in  $x$  must have a tendency to move to an adjacent cell at  $x + \Delta x$  if the concentration at the destination cell is higher than the concentration at  $x$ . In the case of a response to concentrations based on Weber's law, this probability would be given by

$$p(x \rightarrow x + \Delta x) \begin{cases} \gamma \frac{|C(x + \Delta x) - C(x)|}{C(x)}, & \text{if } C(x + \Delta x) > C(x) \\ 0 & \text{otherwise} \end{cases} \quad (4)$$

Considering that there are  $C(x)$  individuals that apply this rule, this will result in a net flow from  $x$  to  $x + \Delta x$  equivalent to  $\gamma(C(x + \Delta x) - C(x))$  if  $x + \Delta x$  is the cell with higher concentration. If instead the cell with higher concentration is the one at  $x$ , particles will flow in the opposite direction, but their flow will turn out to be also proportional to  $\gamma(C(x + \Delta x) - C(x))$ . As a result the net change of density at  $x$  will be:

$$C(x, t + \Delta t) =$$

$$C(x, t) - \gamma [-2C(x, t) + C(x + \Delta x, t) + C(x - \Delta x, t)] \quad (5)$$

whose continuous version is:

$$\frac{\partial C}{\partial t} = -\gamma' \frac{\partial^2 C}{\partial x^2} \quad (6)$$

Equations 5 and 6 are identical to the diffusion equations 1 and 2, except for the sign of the diffusion coefficients  $D$  and  $\gamma$ . Importantly, however, their origin is completely different: the diffusion equation results from the total absence of interactions, while a response based on Weber's law implies an active decision process.

Care should be taken however that the derivation of the anti-diffusion equation 5 from individual-level Weber's law responses (eq. 4) involves some simplifications. First, equation 5 is a mean field approximation of equation 4. Second, if the number of particles or individuals in a cell is close to zero, the probability of these particles

to move to an adjacent higher concentration cell will increase (the denominator of equation 4 is small), but the flow can never exceed the number of available particles. There is no control for this in equation 5, which means that simply applying this equation can potentially lead to some cells taking negative values.

### Restoring arbitrary distributions

Because a response to concentration gradients based on Weber’s law results in a change in concentrations that is analogous to an anti-diffusion, if such a response is implemented by all individuals in a group, it will have the net effect of partially restoring the distribution that was originally altered by diffusion. To visualise this, consider the example in the top row of figure 2. The example depicts the hypothetical case of animals aggregated at two high density spots, with densities close to zero elsewhere (fig. 2-A). Coloured dots mark the positions of randomly selected particles. In the absence of interactions, diffusion operates on densities, which we implement by iterating 300 times a 2D version of equation 1 with parameters  $D = 0.01$ . The superposed particles also move to a random cell adjacent to their current position with probability  $D$ . Figure 2-B shows the resulting density distribution and the trajectories of the selected particles. Applying 300 iterations of anti-diffusion response (a 2D version of equation 5) results in a new spatial distribution (fig. 2-C) where densities are very similar to those in the original distribution.

### An analogy with the problem of deblurring in image processing

Our problem of animals recovering a group configuration that was previously altered by diffusion is closely related to the problem of deblurring in image processing. In fact, a grayscale image can be seen as a density distribution (for instance by assimilating bright colours to high density regions and dark colours to low density regions). Random movements starting from that distribution correspond to blurring the image, and the task of image deblurring algorithms is that of recovering an image similar to the original one. It is well known in the human and computer vision literature that blurred images can be partially restored by subtracting their con-

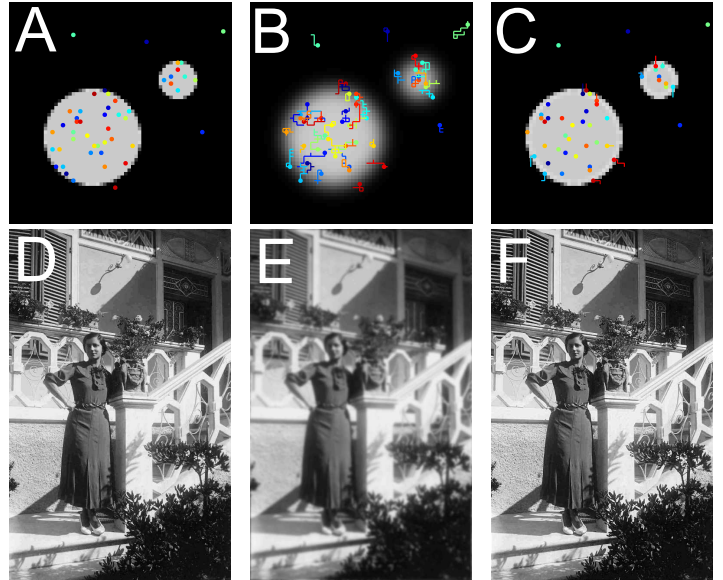


**Figure 2: Weber’s law based anti-diffusion restores spatial distributions after diffusion.** **A** Hypothetical two-dimensional density distribution representing two ‘animal groups’ with a circular profile and homogeneous internal density. The coloured dots indicate the position of randomly selected individuals. After a given number of iterations of random diffusion-like movements (300 in this example), individuals have moved with random trajectories producing a smoothed density distribution (**B**). In **C** a density distribution similar to the original (**A**) distribution is restored by each individual climbing the density gradient with a Weber’s law response rule (parameter  $\gamma = D$  and same number of iterations: 300). Figures **D**, **E** and **F** illustrate an identical process to that in **A**, **B** and **C**, but here the starting density distribution (**D**) is a greyscale image. Random diffusion of the individuals that form the distribution in **D** has the effect of blurring the image (producing the image in **E**) and anti-diffusion restores a similar image to the original (in **F**). In both examples the luminance map is updated based on a mean-field approach (that is, densities are updated in proportion to the calculated probability instead of by actually drawing movement decisions from the probability distribution).

volution with a Laplacian operator, in a similar way to what equation 5 does. In fact, the diffusion equation 2 indicates that the local change in luminance  $\partial C$  when we blur the image by a small amount  $\partial t$  is proportional to the Laplacian of the original image:

$$\frac{\partial C}{\partial t} = D \left[ \frac{\partial^2 C}{\partial x^2} + \frac{\partial^2 C}{\partial y^2} \right] \quad (7)$$

A simple approach for restoring the quality of the initial image is that of playing the diffusion process for negative time scales [18] in a way which is analogous to what is done by equation 5.

Figure 2 D-E illustrates the diffusion and Weber’s law based anti-diffusion applied to a greyscale image. The original image (fig. 2-D) is initially blurred when each of the intensity levels of a pixel randomly diffuses to the neighbouring pixels (fig. 2-E). Implementing a Weber’s law based gradient-climbing response such as the one described in equation 4 restores much of the details that were present in the original image. The only difference between this gradient-climbing approach and classical image deblurring by subtraction of a laplacian convolution is that our approach is based on equation 4, while the convolution with a laplacian implements directly equation 5, which can be derived from it. Unlike gradient climbing, subtracting the laplacian convolution can produce images with negative values; in the context of image processing this is usually resolved by rescaling the image histogram to the allowed range of pixel intensities (e.g. 0-255 for 8 bit images).

## Animal movements within stable density landscapes

The previous examples focused on a somewhat artificial situation whereby particles initially diffuse without interacting and then converge again by implementing a Weber’s law based gradient climbing response.

More realistic is the situation in which a group or a population of animals occupy the environment according to a non-homogeneous density distribution which remains stable over time in spite of individual animals moving across the landscape. Here, we are not making any claims about the actual mechanisms that allow maintaining stable group configurations: these could

involve both inter-attraction among individuals (gregarious behaviour) and attraction to environmental resources that are localised in space.

We model this situation by assuming that animals occupy the environment according to a non-homogeneous density landscape, that for simplicity we map to a discrete lattice. Animals can move from one cell of the lattice to the adjacent cells, but we impose that the density landscape remains unchanged.

Suppose that the number of individuals at two adjacent cells  $i$  and  $j$  is respectively  $N_i$  and  $N_j$  (fig. 3). If the density landscape remains stable,  $N_i$  and  $N_j$  must remain constant over time (and this for all cells, not just for  $i$  and  $j$ ). The easiest way in which this can be achieved is if at any given time the flow  $\phi(i, j)$  from  $i$  to  $j$  is equal to the flow  $\phi(j, i)$  in the opposite direction.

Assuming that  $j$  is the cell with higher density  $N_j > N_i$ , we can say that the individuals that move from  $j$  to  $i$  do it because of diffusion alone, while the individuals that move from  $i$  to  $j$  can do it because of diffusion or because of some form of gradient climbing described by an unknown function  $f(N_i, N_j)$ .

We then have

$$\phi(i, j) = N_i D + N_i f(N_i, N_j) = N_j D = \phi(j, i) \quad (8)$$

which gives

$$f(N_i, N_j) = \frac{D(N_j - N_i)}{N_i} \quad (9)$$

. Weber’s law is hence a solution.

We tested in simulation if particles moving within an overall stable density landscape appear as if they were following Weber’s law response to densities. First, we created a number of 2-dimensional random density landscapes (obtained as low-pass filtered noise). Then, we generated random particle trajectories with the two constraints that (i) the total amount of time spent by a trajectory at a particular location is proportional to the density at that location, and that (ii) at each time step the net flow of particles between two locations is equal to the flow in the opposite direction (see Methods for details; an example of one such density landscape and of some of the corresponding trajectories is illustrated in figure 3-B). The probability of a particle to move

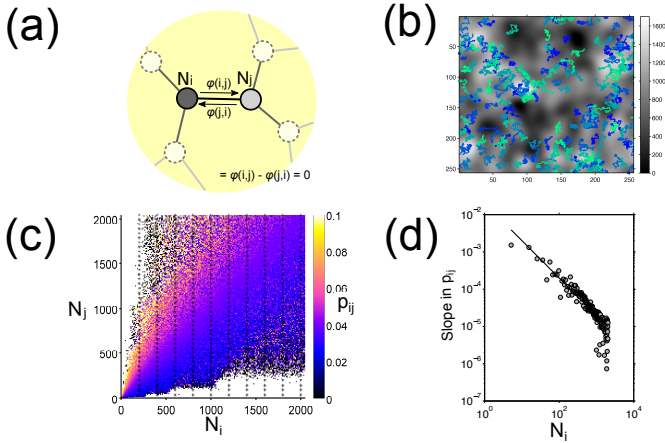


**Figure 3: Flow of individuals across a network of ‘sites’.** (a) The simplest way in which a non flat density landscape can remain stable over time is if the flows of individuals moving across each edge in one direction is balanced by the flow moving in the opposite direction. We built a series of density landscapes such as in (b) whereby each pixel represents a network node and it is directly connected by an edge to its four adjacent pixels. Particles move randomly across the landscape with the constraints that the density distribution is preserved at all times. (c) The probability for a particle to move from node  $i$  to node  $j$  increases linearly with the difference of density between the target  $N_j$  and the source node  $N_i$ . The slope of this relation, obtained from a linear fit along the dotted lines depicted in (c) is inversely proportional to the local density  $N_i$  (panel (d)).

between two adjacent locations calculated over all the trajectories and binned as a function of the local densities at the source location ( $N_i$ ) and at the target location ( $N_j$ ) is illustrated in figure 3-C. While the flow of particles is identical in both directions, individual particles necessarily have a higher probability of moving from low to high density regions. Intuitively, this is easily understood as a consequence of fewer particles being available to counterbalance the flow from adjacent locations. More precisely, the simulated particles responded to local densities with an apparent Weber’s law response, whereby the slope of the probability of moving from  $i$  to  $j$  is inversely proportional to  $N_i$  (fig. 3-D). These simulations show that, no matter if the individuals are attracted to each other or only to environmental features, and no matter what ‘rules of interaction’ with conspecifics they actually implement: as long as the

overall spatial density distribution is maintained, individual group members will appear to respond to their neighbours with a Weber’s law type response.

## Long term dynamics of iterated diffusion and anti-diffusion

While Weber’s law based responses to densities can counteract diffusive forces and are likely to be consistently observed in stable groups with an internal dynamics, can density responses based on Weber’s law alone support group stability? Because of the linearity of the diffusion and anti-diffusion equations (eq. 2 and 6), a combination of diffusion and anti-diffusion has only one equilibrium point with homogeneous density. The homogeneous density state is stable -and the group disperses across the environment- when diffusion is stronger than anti-diffusion (when  $D > \gamma$ ). When instead the anti-diffusion prevails ( $\gamma > D$ ), the homogeneous state becomes unstable and the model predicts the formation of explosively larger groups. In particular, the dynamics of the aggregation is such that the higher spatial frequencies (small spatial scales / small group sizes) are amplified or attenuated faster than lower frequencies (see section 0.6). An important consequence of this is that as soon as the regulation mechanism is noisy, the high frequency noise is quickly amplified.

It is important to remember that in making the considerations above we were relying on two assumptions. The first assumption is that diffusion and anti-diffusion take place simultaneously and the gradient climbing response is perfectly accurate. In reality, if the anti-diffusion response is not implemented immediately the anti-diffusion will take place on a distribution that has already been altered by some uncompensated diffusion. Similarly, if the gradient climbing response is noisy, i.e. it also diffuses a bit, this will also result in some uncompensated diffusion. The second assumption is that local densities can grow with no upper limit. In real world distributions, however, densities will reach a saturation at some point. Here, we incorporate these additional elements in a discrete model of diffusion and anti-diffusion. The model uncouples in time diffusion and anti-diffusion, and implements a saturating anti-

diffusion response to prevent densities from increasing above a saturation point (see methods subsection 0.2).

Under these conditions, we do observe the appearance of spatial patterns of a characteristic scale (see fig. 4).

## Discussion

Weber’s law describes a general functioning principle of sensory systems. Traditionally, Weber’s law based sensory perception has been discussed in relation to the mechanisms and to the constraints of information processing in the brain [19, 20]. Here, we have shown that Weber’s law is also an essential property of collective interactions in stable animal groups.

Sensory perception plays a fundamental role in guiding the interactions of an animal with its environment [21], so it can reasonably be expected that the fundamental properties of sensory systems also play a role in shaping inter-individual interactions and collective behaviour. Previous studies have already established the relevance of decision-making mechanisms based on Weber’s law for explaining collective decision-making in ants, bees and fish [22, 13, 23, 24]. Theoretical studies also indicate that Weber’s law response results from optimal pooling of group-level information for collective decision-making [24].

In the present study, we do not make any assumptions about the mechanisms or about the optimality of the decision-making rules in individual animals. Our only assumption is that animal groups remain stable over long time scales, compared to the time scale of individual animal movements. We further assumed that in the absence of interactions, individual animal movements are independent from local densities and group dynamics is described by diffusion. Because of the generality of these assumptions, we can conclude that Weber’s law response to animal densities is a general property of all stable groups.

We should however be careful not to conclude that all animal aggregation phenomena depend on Weber’s law based responses to neighbour densities. Many animal aggregations can be produced also in the complete absence of social interactions and of gregarious behaviour. This is the case for instance when animals are attracted to an environmental feature such as a source of water or

a particular type of vegetation. In this case, group stability would be predominantly mediated by the external attractor. Yet, our analysis shows that if we erroneously consider that the attraction responses are directed to other group members and not to the environmental feature, also in this case we would observe a response in the form of a Weber’s law to neighbour densities. In some animal species, group members might implement different response rules, involving both inter-individual attraction and repulsion. As long as the overall effect of these interactions is that of keeping the group stable, we would observe a Weber’s law type of response to neighbour densities, without it necessarily being the underlying mechanism.

Our model is not a morphogenetic model: the type of response to neighbour densities based on Weber’s law that we describe here cannot be used to predict the size or the shape of the groups formed by animals of a particular species. We argue that this is an inevitable consequence of the ‘universality’ of Weber’s law: animal groups present a huge variation of size and shape across species which is unlikely to be accounted for by a single shared perceptual rule. In addition, the size of animal groups is typically widely distributed also within one single species, suggesting that its regulation depends on other factors, such as merge and split phenomena, rather than being determined by sensory responses alone [25, 26, 27].

While we do actually show that an aggregation model based on Weber’s law can lead to the formation of patterns at a fixed scale, this scale is mainly determined by the delay that we introduced between diffusion and anti-diffusion. It is implicit in the nature of the diffusion equation that the introduction of events with a characteristic temporal scale -for instance a fixed reaction time in the response to neighbours, also leads to the appearance of spatial patterns with a characteristic scale. For this reason we are quite confident that this kind of pattern formation is not an artifact of our simplified model. We could try to find a resemblance between the patterns produced in our long-term iteration model and the spatial distribution of individuals in certain animal groups, such as for instance mussel beds[1]. However, we think that it is safer to argue that these pattern formation phenomena at a very small spatial scale have little

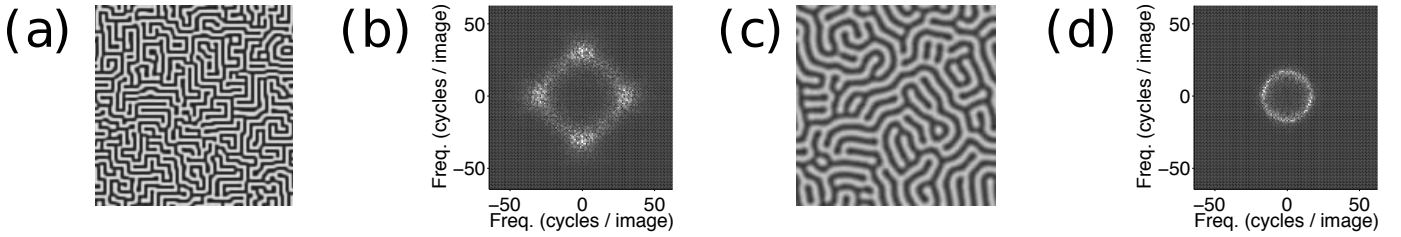


**Figure 4: Pattern formation from iterated diffusion and anti-diffusion.** (a) and (c) Spatial patterns produced on a 128x128 lattice after 15000 iterations of the model described in 0.2; the starting distribution is random white noise. In both figures  $\gamma = 0.9$ . In (a)  $D = 0.13$ , while in (b)  $D = 0.17$ . After multiple iterations of the simulation steps, a pattern emerges at a single spatial scale. This is clearly visible in figures (b) and (d), which plot the amplitude spectrum of the Fourier transform of the patterns in (a) and (c), respectively.

biological relevance in general, for instance because at such small spatial scales the positioning of individuals is more affected by direct individual to individual interactions than by the generic Weber’s law response that we consider here.

Our study points to a general relation between Weber’s law and collective behaviour. While Weber’s law can explain several perceptual phenomena, there are many instances in which sensory perception deviate from Weber’s law behaviour. Future studies should try to relate also deviations from Weber’s law, as well as other perceptual phenomena, to collective behaviour. For example, many sensory stimuli remain undetected when their intensity falls below a perception threshold. In the context of social interactions, perceptual thresholds for responding to conspecifics can directly affect the way how animals rely on private vs. social information for taking decisions.

Our approach of deriving interaction rules from the observation of the typical configuration of a group and from simple assumptions about how noise acts on the system is complementary to the direct observations of interacting individuals. In fact, while direct observations of behaviour inform us about how animals of a particular species interact, our approach informs us about which forms of interactions are an inevitable feature of all behaviours resulting in a particular collective phenomenon. We are confident that in future our approach can be extended to the study of also other more complex forms of group coordination.

## Methods

### 0.1 Movements in a stable density landscape

In order to explore the interaction responses compatible with maintaining a stable density landscape we first created random density landscapes and then we simulated movements of particles over the landscape while imposing that the flows of particles in alternate directions over each edge is balanced for each time step.

The random density landscape was obtained as low-pass filtered two-dimensional random noise (through convolution with a Gaussian distribution). We tested multiple landscapes with different values of average density, amplitude of modulation and spectral composition.

The probability for an individual particle to move from a cell  $i$  to an adjacent cell  $j$  was calculated as follows: first we calculated the flows of particles that would move from  $i$  to  $j$  through diffusion alone,  $F_{ij}^{fwd} = DN_i$ . Then we immediately compensated these flows by moving an identical number of particles in the opposite direction. These particles are selected randomly among those available in  $j$  and could be the same that had just moved from  $i$  to  $j$  with probability  $F_{ij}^{fwd} / (F_{ij}^{fwd} + N_j)$ . As a result, the net flow of particles that moved from  $i$  to  $j$  because of diffusion and were not put back during the compensatory step is  $FD_{ij} = F_{ij}^{fwd} - (F_{ij}^{fwd})^2 / (F_{ij}^{fwd} + N_j)$ , and it is associated with a net compensatory flow from  $j$  to  $i$ ,  $FC_{ji} = FD_{ij}$ . By imagining that the same process also takes place in the opposite direction, with diffusion from  $j$  to  $i$ , and a compensatory movement from  $i$  to  $j$ , the total flow between  $i$  and  $j$  is  $FD_{ij} + FC_{ij}$ .

## 0.2 Long-term dynamics of iterated diffusion and anti-diffusion

We implemented a simulation in which an initial density distribution is altered by alternating steps of diffusion and anti-diffusion in discretised time steps. The first step is a simple diffusion step:

$$C(x, y, t + 1) = C(x, y, t) + D \Delta (C(x, y, t)) \quad (10)$$

where

$$\Delta (C(x, y, t)) = -4C(x, t) + C(x + 1, y, t) + C(x - 1, y, t) + C(x, y + 1, t) + C(x, y - 1, t) \quad (11)$$

The anti-diffusion step is similar to all previous examples, but we also include an additional term to prevent densities from becoming negative, or from exceeding a maximum positive value.

$$C(x, y, t + 2) = C(x, y, t + 1) - \gamma \Delta (C(x, y, t + 1)) \quad (12)$$

In the examples shown in figure 4 the initial condition is a uniform random distribution. And the distribution shown corresponds to 15000 simulation steps.

## Appendix

### 0.3 Derivation of the continuous diffusion equation

The continuous diffusion equation 2 can be derived from the discrete equation 1 by considering the Taylor series approximation of  $C(x, t + \Delta t)$  around  $C(x, t)$ :

$$C(x, t + \Delta t) = C(x, t) + \Delta t \frac{\partial C}{\partial t} + \dots$$

and the Taylor series approximation of  $C(x + \Delta x, t)$  around  $C(x, t)$ :

$$C(x + \Delta x, t) = C(x, t) + \Delta x \frac{\partial C}{\partial x} + \frac{(\Delta x)^2}{2} \frac{\partial^2 C}{\partial x^2} + \dots$$

When these are plugged into equation 1, the first spatial derivatives cancel each other out and the remaining equation is  $\Delta t \frac{\partial C}{\partial t} = D(\Delta x)^2 \frac{\partial^2 C}{\partial x^2}$ . We then collect the parameters  $\Delta t$ ,  $D$  and  $(\Delta x)^2$  into a new constant  $D'$ .

### 0.4 A training problem: recovering Gaussian distributions

Imagine to release a certain number of animals at a single location ( $C(x, 0)$  is a delta function). Equation 3 tells us that, in the absence of *any* interactions, after some time  $t$  the individuals will be distributed according to a Gaussian distribution  $G$  centered around the release point and whose variance is proportional to  $t$ .

One first question that we can ask is, what kind of movement response would allow the group to temporarily contrast the spreading process and revert from the spatial distribution that was produced at time  $t$  to the distribution that existed before, at time  $t - \Delta t$  (fig. 5)

In this simple case comes to our help the fact that we just want to convert a Gaussian distribution (the distribution at time  $t$ ; dotted distribution in figure 5) into another Gaussian distribution (that existed at some previous time  $t - \Delta t$  (shaded distribution in figure 5). The simplest way in which this can be achieved is if each individual moves towards the direction of higher local density by an amount  $\Delta x$  proportional to its own current distance  $x$  from the centre of the distribution.

In practice, however, we should assume that individuals do not have a global perception, that is, they do not know directly their own position relative to the centre of the distribution. They can, however, estimate the number of neighbours locally around their own position and its local variation in different directions. In the case of Gaussian distributions, it is easy to verify that there is one function of these local quantities that is proportional to the distance from the centre of the distribution: this is the gradient normalized over the local density  $x = -\frac{\nabla G}{G} \sigma^2$ , where  $\nabla G = \frac{\partial G}{\partial x}$  indicates the gradient of the Gaussian distribution (because  $\frac{\partial G}{\partial x} = -\frac{x}{\sigma^2} G$ ). Expressions of the form  $\frac{\nabla f}{f}$  are well known in psychophysics and correspond to Weber's law.

### 0.5 Internal movements within a Gaussian probability landscape that remains stable over time

Here we consider a Gaussian distribution stable over time, but assuming that individuals move freely within this distribution, that is, the global distribution does not

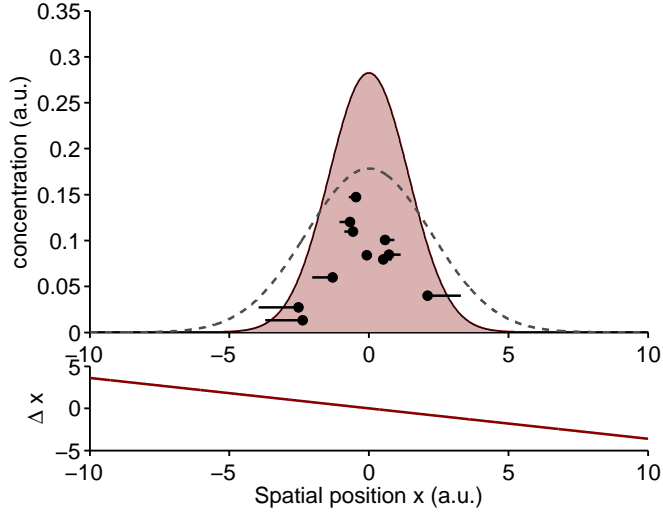


**Figure 5: Individual movements to contrast gaussian diffusion.** We consider the simple example of individuals distributed across space according to a Gaussian density distribution. If each individual aims at recovering

change, but there are internal movements inside this distribution.

For each individual we simulate Normally distributed  $x$  positions with time correlation.

Notice that the slope of the regression line is not 1 but  $2/\pi$ . This results from attenuation and the value of the slope is related to the average absolute deviation of the Normal distribution, which is  $\sqrt{2/\pi}$ .

## 0.6 Amplification and attenuation of different spatial harmonics around the homogeneous state

We consider the evolution of  $C$  around an homogeneous steady state where a small perturbation  $\delta$  is applied:  $C(x, t) = C_s + \delta(x, t)$ . We choose a form for  $\delta = e^{\omega t} e^{ikx}$  which allows us monitoring the temporal and spatial evolution of the perturbation.

If diffusion and anti-diffusion act simultaneously, we have:

$$\frac{\partial C}{\partial t} = +D \frac{\partial^2 C}{\partial x^2} - \gamma \frac{\partial^2 C}{\partial x^2} \quad (13)$$

The equation implies an immediate response of individuals to the diffusion event, so that in practice it is equivalent to a slower diffusion (if  $D > \gamma$ ) or slow anti-diffusion (if  $\gamma > D$ ).

The time derivative in equation 13 can be rewritten around the homogeneous state as  $\frac{\partial C}{\partial t} = \left( \frac{\partial C_s}{\partial t} + \frac{\partial \delta(x,t)}{\partial t} \right)$ , and similarly for the space derivative  $\frac{\partial^2 C}{\partial x^2} = \left( \frac{\partial^2 C_s}{\partial x^2} + \frac{\partial^2 \delta(x,t)}{\partial x^2} \right)$ . As the derivative of the constant parts are equal to zero, equation 13 around the homogeneous state becomes

$$\frac{\partial \delta}{\partial t} = (D - \gamma) \frac{\partial^2 \delta}{\partial x^2}$$

from which we have  $\omega \delta = (D - \gamma) - k^2 \delta$  which indicates that the speed  $\omega$  at which harmonics of a given frequency  $k$  are amplified or attenuated (depending on the sign of  $D - \gamma$ ) is proportional to the square of the frequency: high frequency harmonics are both amplified faster when anti-diffusion prevails and attenuated faster when diffusion prevails.

## References

- [1] van de Koppel J, et al. (2008) Experimental evidence for spatial self-organization and its emergent effects in mussel bed ecosystems. *Science* 322:739–742.
- [2] Puckett JG, Kelley DH, Ouellette NT (2014) Searching for effective forces in laboratory insect swarms. *Scientific Reports* 4:4766–.

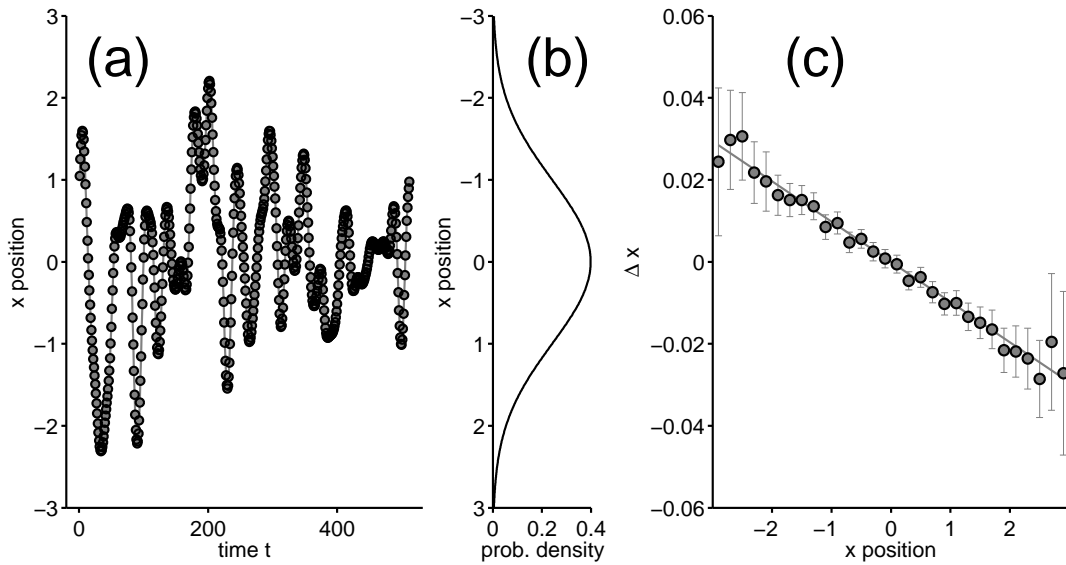


**Figure 6: Apparent Weber’s law response of randomly moving particles in a Gaussian density distribution.** (a) Simulated  $x$  position of a particle that moves randomly across a Gaussian probability landscape depicted in (b). (c) Average movement ( $\pm$  standard deviation) of the particle as a function of its current position. Individual particles are observed to move towards the centre of the distribution with a step

- [3] Devigne C, Broly P, Deneubourg JL (2011) Individual preferences and social interactions determine the aggregation of woodlice. *PLoS ONE* 6:1–12.
- [4] Krause J, Ruxton G (2002) *Living in groups* (Oxford University Press, USA).
- [5] Ballerini M, et al. (2008) Interaction ruling animal collective behaviour depends on topological rather than metric distance: Evidence from a field study. *Proc Natl Acad Sci U S A* 105:1232–1237.
- [6] Herbert-Read JE, et al. (2011) Inferring the rules of interaction of shoaling fish. *Proc Natl Acad Sci U S A* 108:18726–18731.
- [7] Gautrais J, et al. (2012) Deciphering interactions in moving animal groups. *PLoS Comput Biol* 8:e1002678.
- [8] Strandburg-Peshkin A, et al. (2013) Visual sensory networks and effective information transfer in animal groups. *Current Biology* 23:R709–R711.
- [9] Attanasi A, et al. (2014) Information transfer and behavioural inertia in starling flocks. *Nature physics* 10:615–698.
- [10] Herbert-Read JE, Buhl J, Hu F, Ward AJW, Sumpter DJT (2015) Initiation and spread of escape waves within animal groups. *Open Science* 2.
- [11] Weber EH (1834) *De pulsu, resorptione, auditu et tactu. Annotationes anatomicae et physiologicae* (Koehler, Leipzig).
- [12] Anobile G, Cicchini GM, Burr DC (2016) Number as a primary perceptual attribute: A review. *Perception* 45:5–31.
- [13] von Thienen W, Metzler D, Choe DH, Witte V (2014) Pheromone communication in ants: a detailed analysis of concentration-dependent decisions in three species. *Behavioral ecology and sociobiology* 68:1611–1627.
- [14] Agrillo C, Dadda M, Serena G, Bisazza A (2008) Do fish count? spontaneous discrimination of quantity

- in female mosquitofish. *Animal Cognition* 11:495–503.
- [15] Ditz HM, Nieder A (2016) Numerosity representations in crows obey the weber–fechner law. *Proceedings of the Royal Society of London B: Biological Sciences* 283.
- [16] Jordan KE, Brannon EM (2006) Weber’s law influences numerical representations in rhesus macaques (*macaca mulatta*). *Animal cognition* 9:159–172.
- [17] Fick A (1855) On liquid diffusion. *Poggendorffs Annalen* 94:59 reprinted in *Journal of Membrane Science* 100: 33-38, 1995.
- [18] ter Haar Romeny BM, Florack LM, Salden AH, Viergever MA (1993) *Higher order differential structure of images* (Springer Berlin Heidelberg), pp 77–93.
- [19] Jacob SN, Vallentin D, Nieder A (2012) Relating magnitudes: the brain’s code for proportions. *Trends in cognitive sciences* 16:157–166.
- [20] van Hateren JH (1992) A theory of maximizing sensory information. *Biological cybernetics* 68:23–29.
- [21] Akre KL, Johnsen S (2014) Psychophysics and the evolution of behavior. *Trends in Ecology & Evolution* pp –.
- [22] Perna A, et al. (2012) Individual rules for trail pattern formation in argentine ants (*linepithema humile*). *PLoS Comput Biol* 8:e1002592.
- [23] Reina A, Bose T, Trianni V, Marshall JA (2018) Psychophysical laws and the superorganism. *Scientific reports* 8:4387.
- [24] Arganda S, Pérez-Escudero A, de Polavieja GG (2012) A common rule for decision making in animal collectives across species. *Proc Natl Acad Sci U S A* 109:20508–20513.
- [25] Bonabeau E, Dagorn L, Fron P (1999) Scaling in animal group-size distributions. *Proc Natl Acad Sci U S A* 96:4472–4477.
- [26] Niwa HS (2004) Space-irrelevant scaling law for fish school sizes. *J Theor Biol* 228:347–357.
- [27] Ma Q, Johansson A, Sumpter DJ (2011) A first principles derivation of animal group size distributions. *Journal of theoretical biology* 283:35–43.